

# A primary pressure standard at 100 kPa

*J. W. Schmidt, Yueqin Cen, R. G. Driver,  
W. J. Bowers, J. C. Houck, S. A. Tison  
and C. D. Ehrlich*

**Abstract.** Primary pressure standards in the atmospheric pressure range are often established using mercury manometers. To a lesser extent, controlled-clearance dead-weight testers, in which one component (normally the piston) has been dimensionally measured, have also been used. The recent advances in technology on two fronts: (i) the fabrication of large-diameter pistons and cylinders with good geometries; and (ii) the dimensional metrology capability of these components, have allowed some dead-weight testers at the National Institute of Standards and Technology (NIST) to achieve total relative uncertainties ( $2\sigma$ ) in generated pressure near  $10 \times 10^{-6}$  (10 ppm). This paper describes recent developments at the NIST in which accurate dimensional measurements have been translated into effective areas. It is anticipated that total relative uncertainties in generated pressure may decrease to 5 ppm ( $2\sigma$ ) when recent dimensional measurements are incorporated in the newest gauges.

## 1. Introduction

Traditional calibration paths for dead-weight testers in the atmospheric pressure range were often based on mercury manometry [1-3]. A second path relied on dimensional measurements of the piston, together with controlled-clearance piston gauge theory as presented by Heydemann and Welch [4], to obtain a characterization of the effective area of the gauge in operation. Dimensional measurements of the cylinder at the accuracy needed to be competitive with manometry were unavailable, partly because of the small size of the cylinders and the difficulty in getting probes inside the bores. The Pressure and Vacuum Group at the NIST has recently acquired a new generation of dead-weight testers that operate in a pressure range between 30 kPa and 175 kPa. The new gauges have large diameters ( $\sim 50$  mm) which allow the diameters of each piece, the piston and the cylinder, to be measured with an uncertainty of 50 nm ( $1\sigma$ ,  $k = 1$ ). This measurement accuracy, in particular of the cylinder, allows a more direct determination of the effective areas of these gauges and allows one to bypass the Heydemann-Welch method, which involves an extrapolation of the piston fall-rate data (a measure of the crevice width)

for part of its analysis. This extrapolation in turn makes it difficult to estimate the uncertainty of the effective area in specific cases. Of course, while the present approach is free from extrapolations it is not completely model-independent, but in favourable cases the differences in effective area between estimates from two competing models (a viscous-flow model and an interpolated molecular-viscous flow model) is less than 2.5 ppm.

The principle developments in this field arise from improvements in the ability of manufacturers to make 35 mm and 50 mm diameter pistons and cylinders that are reproducible. Several gauges of the 50 mm ceramic type with effective areas within 5 ppm of each other have been studied extensively by Simpson and Clow [5]. In this paper we describe an extension of their work but with a tungsten-carbide piston that eliminates possible electrostatic charging effects. In future work we will concentrate on a 50 mm gauge in which both piston and cylinder are made from tungsten carbide.

## 2. Apparatus

The present apparatus consists of a single stationary tungsten-carbide (WC) piston, 50 mm in diameter, and a floating cylinder [6]. The cylinder, made from a ceramic material (CER), was placed over the stationary piston. The gauge was designed so that the stationary piston (itself a hollow cylinder) could be expanded with an independent control pressure if desired. This combination is designated PG-201-WC/CER to distinguish it from its predecessor, PG-201-CER/CER, in which both piston and cylinder were made from a

J. W. Schmidt, Yueqin Cen,<sup>1</sup> R. G. Driver, W. J. Bowers, J. C. Houck, S. A. Tison<sup>2</sup> and C. D. Ehrlich:<sup>3</sup> Process Measurements Division, National Institute of Standards and Technology (NIST), Gaithersburg, MD 20899, USA.

1. Guest Researcher from the National Institute of Metrology, Beijing, People's Republic of China.

2. Currently at Millipore Corp., Dallas, Texas.

3. Technical Standards Activities Program, NIST.

ceramic material. The cylinder height and the rotation speed could also be monitored by *in situ* proximity sensors and a counter. A sensitive differential pressure cell and a separate piston gauge were used to transfer pressures to the calibration chain of the Pressure and Vacuum Group, perform consistency checks and compare with historical values.

### 3. Measurements

The dimensional measurements were of three types: (i) roundness; (ii) straightness; and (iii) diameter. The roundness and straightness measurements were relative while the diameter measurements were absolute. A full complement of dimensional measurements was made on the 50 mm WC piston and the 50 mm CER cylinder, and it is planned that a full complement of measurements will be made on a WC cylinder after new control hardware and software is installed in the dimensional measurement equipment [7].

The roundness measurements were made at five latitudes, 8 mm apart. Each of the five measurements was actually a composite of twelve roundness traces at 1° increments indexed by 30°. In this way, some uncertainties introduced by the measurement system and associated with the azimuth were removed. The straightness measurements were made at 0.5 mm increments along eight longitudes separated by 45°. Each straightness trace was made twice, indexed by 180° with respect to each other. In this way, other uncertainties associated with the vertical axis of the measurement system were removed. Finally, three diameters along the directrix, separated by 8 mm, were measured. These measurements were made in the 0°/180° plane and another three were made in the 90°/270° plane, giving a total of six diameters on each piece.

The dimensional measurements were converted to effective area in two ways:

- (a) a direct average of the twelve diameters within the engagement area (six from the piston and six from the cylinder);
- (b) a numerical integration of the surface forces acting over the reconstructed surface [8].

Method (b) assumed viscous flow of the pressurizing gas (nitrogen) through the crevice. The crevice profile,  $h(z)$ , was taken to be the crevice width averaged over the azimuth at each height,  $h_{ave}(z)$ . Other crevice profiles were used, including the maximum width at each height,  $h_{max}(z)$ .

A solution using finite element analysis for the three-dimensional flow is anticipated. This is expected to yield values for the effective areas that fall between the two solutions corresponding to  $h(z) = h_{ave}(z)$  and  $h(z) = h_{max}(z)$ .

In addition to using dimensional measurement as a method of obtaining an effective area, auxiliary

measurements of fall rate and spin rate were made as consistency checks of the dimensional measurements. Both types of auxiliary measurement were used to estimate crevice widths. The fall-rate measurements yield the moment  $\langle 1/h^3(z) \rangle$  while the spin-rate decrements yield the moment  $\langle 1/h(z) \rangle$ . For crevices that are uniform over the piston/cylinder engagement surface, the two measurements should be related:  $\langle 1/h^3(z) \rangle = \langle 1/h(z) \rangle^3$ . The elastic response of the piston to control pressure was also measured and compared with the elastic response calculated from the thick-walled formula from elasticity theory, which uses the material properties, Young's modulus and Poisson's ratio. Finally, the following rather significant aerodynamic effect was observed and then quantified by two of the authors, RGD and WJB.

In operation, the gauge was found to exhibit a measurable aerodynamic effect in the gauge mode that influenced the pressures generated by the gauge. This effect was first observed by Prowse and Hatt [9], later by Sutton [10], and then by Tilford and Hyland [11]. Further research could be carried out in this regard but the present results indicate the existence of a small force that is proportional to the square of the rotation frequency. This effect has been shown by Sutton to arise from the swirling of the air in the bell jar covering the gauges. The layer of air in the bell jar, which is located next to the top surface of the weights, circulates out horizontally across the weights, up the sides of the bell jar and returns downwards along the axis. As Sutton noted, this last step (the downward flow of air in the centre) produces an increase in the total force acting downwards on the gauge. The effect is observed as a pressure increase generated by the gauge or a decrease in the gauge's effective area. As Prowse and Hatt noted, this force in general will depend on the presence or absence of a bell jar and on the diameter of the weights. Tilford and Hyland showed the effect to be proportional to the density of the gas in the bell jar.

### 4. Results

The resulting effective area at zero-extrapolated load,  $A_0$ , was calculated from the dimensional measurement in two ways:

- (a) by direct average of the diameters;
- (b) by numerical integration of forces over the surface of the cylinder.

As a consistency check on the dimensions, the fall rates and spin-rate decrements were measured. These yield independent (although imperfect) estimates of the crevice width. The pressure coefficient,  $\lambda$ , was estimated based on elasticity theory and approximate boundary conditions applied to both piston and cylinder. The aerodynamic effect resulting from rotation speed was measured using a transfer gauge.

**Table 1.** Measured diameters at  $T = 20\text{ }^\circ\text{C}$ . Uncertainties are indicated with a coverage factor  $k = 1$ .

$d_0/\text{mm}$	$d_{90}/\text{mm}$	$\langle d \rangle_{\text{ave}, 0 + 90}/\text{mm}$	Relative standard uncertainty $\times 10^6$		
			Type A	Type B	Total
<i>WC piston</i>					
49.968 736	49.968 771	49.968 754			
49.968 683	49.968 708	49.968 696			
49.968 675	49.968 654	49.968 664			
$\langle d_p \rangle_{\text{ave}}$		<b>49.968 704</b>	<b><math>\pm 0.35</math></b>	<b><math>\pm 0.98</math></b>	<b><math>\pm 1.04</math></b>
<i>CER cylinder</i>					
49.970 595	49.969 660	49.970 128			
49.970 080	49.969 710	49.969 895			
49.969 850	49.969 975	49.969 912			
$\langle d_c \rangle_{\text{ave}}$		<b>49.969 978</b>	<b><math>\pm 3.0</math></b>	<b><math>\pm 1.02</math></b>	<b><math>\pm 3.2</math></b>

### 4.1 Dimensional measurements

#### 4.1.1 $A_0$ derived from direct average of diameters

The dimensional measurements of the WC piston and the CER cylinder are listed in Table 1. The uncertainties are total standard uncertainties ( $1\sigma$ ,  $k = 1$ ).

The effective area,  $A_0$ , of the gauge at zero pressure was obtained from the average diameters  $\langle d_p \rangle$  and  $\langle d_c \rangle$  of the piston and cylinder, respectively, from the equation

$$A_0 = \pi(\langle d_p \rangle^2 + \langle d_c \rangle^2)/8. \quad (1)$$

Table 2 gives the value of  $A_0$  from this calculation. The uncertainty represents the total standard uncertainty.

**Table 2.** Effective area,  $A_0$ , of PG-201-WC/CER at  $T = 20\text{ }^\circ\text{C}$  and zero load. Uncertainties are indicated with a coverage factor  $k = 1$ .

Direct average of diameters	$A_0 = 1961.088 (1 \pm 4.6 \times 10^{-6}) \text{ mm}^2$
Numerical integration of surface forces	$A_0 = 1961.083 (1 \pm 4.5 \times 10^{-6}) \text{ mm}^2$

The ceramic cylinder has been measured once before, in 1993 [12]. A comparison of the present measurements with those of 1993 indicates some change in shape over time. In general, the previous values show better roundness than the present values. The average diameter has remained fairly constant, however, within ( $1.6 \times 10^{-6}$ )  $\langle d_c \rangle$ . We believe this is because a positive distortion in the diameter on one longitude creates a negative distortion in the diameter on the longitude  $90^\circ$  away.

#### 4.1.2 $A_0$ derived from numerical integration of surface forces

The three types of dimensional measurement, diameter, straightness and roundness, were combined to form a scaffold of measurements defining the surface of both piston and cylinder. With these measurements, totalling 2376 locations, it was possible to determine the surface

profile for each object with an uncertainty of 100 nm ( $1\sigma$ ,  $k = 1$ ). All of the data taken together yielded a redundant (over-constrained) set of data. We found that the average dimensional mismatch because of the redundancy was 29 nm for the cylinder and 41 nm for the piston. Smooth analytical functions were used to represent the surface over which forces acted. The effective area,  $A_0$ , from this calculation is also listed in Table 2, where the uncertainty represents the total standard uncertainty.

### 4.2 Auxiliary measurements

The crevice width can be estimated independently using the fall-rate and spin-rate decrement methods. The fall-rate method yielded the crevice width  $h \approx 950$  nm, while the spin-rate decrement method yielded the value  $h \approx 700$  nm. Both values were obtained under conditions of system pressure  $p = 175$  kPa and clearance-control pressure  $p_{CC} = 0$  Pa. We believe that these two values of  $h$  differ from one another and from the value obtained from dimensional measurements ( $h \approx 637$  nm) because the cylinder exhibited a significant height-dependent eccentricity determined from dimensional measurements:

$$\varepsilon(z) = (3 + 0.375 z/\text{mm}) \times 10^{-6},$$

while the models used for the analysis of fall rates and spin-rate decrements assumed perfect symmetry.

### 4.3 Pressure coefficient

The pressure coefficient,  $\lambda$ , was estimated based on elasticity theory, which uses Young's modulus, Poisson's ratio and approximate boundary conditions applied to both piston and cylinder. Although we could not verify experimentally our estimates for  $\lambda$  in detail, we were able to check a related quantity, the Heydemann-Welch parameter  $d = (1/A)dA/dp_{CC}$ . The parameter  $d$  was checked using the fall-rate method and the application of a controlled-clearance pressure,  $p_{CC}$ , on the inside of the piston. The value of  $d$  calculated from elasticity theory agreed with the measured value

$(3.21 \times 10^{-12} \text{ Pa}^{-1})$  within  $0.15 d$  [ $\lambda_{\text{theory}} = (6.80 \pm 0.68) \times 10^{-12} \text{ Pa}^{-1}$  ( $k = 1$ ) in re-entrant mode ( $p_{\text{CC}} = p_{\text{load}}$ ) and  $(3.75 \pm 0.38) \times 10^{-12} \text{ Pa}^{-1}$  ( $k = 1$ ) in simple mode ( $p_{\text{CC}} = p_{\text{atm}}$ )].

#### 4.4 Aerodynamic effect

The aerodynamic effect to which we referred in Section 3 was quantified by cross-floating PG-201-WC/CER against a transfer gauge (see Figure 1). The change in pressure was measured as a function of rotation rate and rotation direction. PG-201-WC/CER was operated at rotation rates between 0.33 Hz and 1.33 Hz (clockwise) and between  $-0.33$  Hz and  $-1.33$  Hz (counter-clockwise). All masses used in these measurements had the same diameter (235 mm) and the bell jar contained air. For all loads under the conditions described above, the pressure increase was found to be proportional to the square of the rotation rate;  $\delta p = a f^2$ , where  $a$  was found to be  $(0.35 \pm 0.01) \text{ Pa/Hz}^2$  ( $k = 1$ ). The transfer gauge was always operated at a low rotation rate in order to minimize any aerodynamic effect present in the transfer gauge.

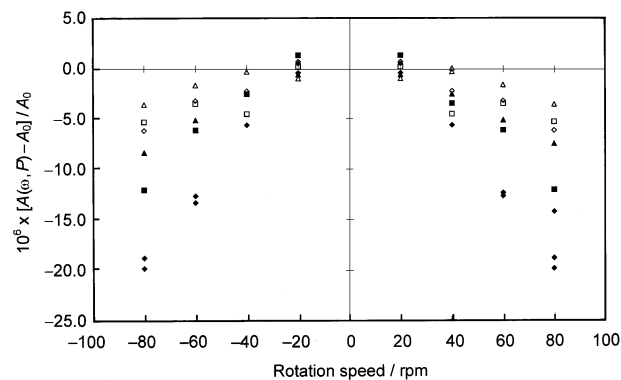


**Figure 1.** Change in effective area versus rotation speed of PG-201 (50 mm WC/CER) in gauge mode. The symbols indicate different loads:  $\blacklozenge$  32 kPa;  $\blacksquare$  52 kPa;  $\blacktriangle$  77 kPa;  $\diamond$  102 kPa;  $\square$  127 kPa;  $\triangle$  152 kPa.

#### 5. Summary

Both piston and cylinder of a large-diameter, 50 mm, dead-weight tester (PG-201-WC/CER) have been dimensionally measured. The measurements have been

converted to an effective area with no load,  $A_0$ , using a numerical integration over the surface of the piston and cylinder. When a pressure term,  $\lambda p$ , in which  $\lambda$  is based on elasticity theory, and a measured aerodynamic term,  $a f^2$ , are both included, then the effective area can be described by the following equation:

$$A_{\text{eff}}(p, \omega) = A_0 \left( 1 + \lambda p + a \frac{f^2}{p} \right). \quad (2)$$

Here,  $A_0$  is the integrated value  $(1961.083 \pm 0.009) \text{ mm}^2$ ,  $\lambda = (3.75 \pm 0.19) \times 10^{-12} \text{ Pa}^{-1}$  and  $a = (-0.35 \pm 0.01) \text{ Pa/Hz}^2$ .

PG-201-WC/CER was used to calibrate a solid WC/WC transfer gauge known within the NIST as PG-28. Table 3 gives the resulting effective areas of PG-28 referred to a temperature of  $23^\circ\text{C}$ . For comparison, Figure 2 gives the previous values from the gas thermometer manometer (GTM) in absolute mode, and the ultrasonic interferometric manometer (UIM) in gauge and absolute modes. The values show a spread of 10 ppm with that of the UIM (absolute mode, 1989) being the highest and that of the UIM (absolute mode, 1996) being the lowest. The present value, based on the numerically integrated value of PG-201-WC/CER

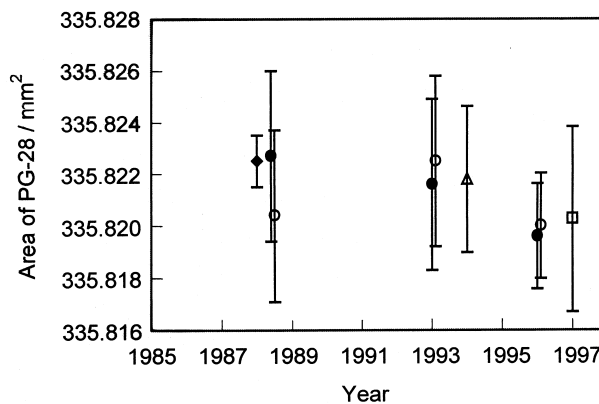


**Figure 2.** Ten-year history of calibrations of PG-28. The bars indicate total uncertainty with coverage factor  $k = 2$ . Generated pressure is about  $10^5 \text{ Pa}$ . The calibration by the 50 mm WC/CER (gauge mode) is shown as  $\square$ ; the 50 mm CER/CER (gauge mode) as  $\triangle$ ; the gas thermometer manometer (1988) as  $\blacklozenge$ ; the ultrasonic interferometric manometer (absolute mode  $\bullet$ , gauge mode  $\circ$ ).

**Table 3.** Effective areas of PG-28 at  $T = 23^\circ\text{C}$  and  $P = 10^5 \text{ Pa}$ . Uncertainties are indicated with a coverage factor  $k = 2$ .

Apparatus	Date of measurement	Effective area
GTM (absolute)	1988	$A_{\text{eff}} = 335.8225 (1 \pm 1.0 \times 10^{-6}) \text{ mm}^2$
UIM (absolute)	1989	$A_{\text{eff}} = 335.8227 (1 \pm 10.0 \times 10^{-6}) \text{ mm}^2$
(gauge)	1989	$A_{\text{eff}} = 335.8204 (1 \pm 10.0 \times 10^{-6}) \text{ mm}^2$
(absolute)	1993	$A_{\text{eff}} = 335.8216 (1 \pm 10.0 \times 10^{-6}) \text{ mm}^2$
(gauge)	1993	$A_{\text{eff}} = 335.8225 (1 \pm 10.0 \times 10^{-6}) \text{ mm}^2$
(absolute)	1996	$A_{\text{eff}} = 335.8196 (1 \pm 6.0 \times 10^{-6}) \text{ mm}^2$
(gauge)	1996	$A_{\text{eff}} = 335.8200 (1 \pm 6.0 \times 10^{-6}) \text{ mm}^2$
PG-201-CER/CER (gauge) [13]	1994	$A_{\text{eff}} = 335.8218 (1 \pm 8.4 \times 10^{-6}) \text{ mm}^2$
PG-201-WC/CER (gauge)	1997	$A_{\text{eff}} = 335.8203 (1 \pm 10.6 \times 10^{-6}) \text{ mm}^2$

(gauge mode), is about 6 ppm below that of the GTM (absolute mode) and about 1 ppm above that of the UIM (gauge mode, 1996). Using the direct average value for PG-201-WC/CER would shift the value for PG-28 closer to the GTM (absolute-mode) value by about 2.5 ppm.

**Acknowledgements.** The authors thank David Simpson and Phil Clow of the National Physical Laboratory for initial numerical calculations of the ceramic pistons and cylinders, and John Stoup of the NIST Precision Engineering Division for the dimensional measurements. We also thank Charles Tilford for data referenced to the UIM.

## References

1. Guildner L. A., Stimson H. F., Edsinger R. E., Anderson R. L., *Metrologia*, 1970, **6**, 1-18.
2. Welch B. E., Edsinger R. E., Bean V. E., Ehrlich C. D., High Pressure Metrology, *BIPM Monographie 89/1*, 1989, 81-94.
3. Tilford C. R., Hyland R. W., Yi-Tang S., High Pressure Metrology, *BIPM Monographie 89/1*, 1989, 105-113.
4. Heydemann P. L. M., Welch B. E., In *Experimental Thermodynamics, Vol. II: Experimental Thermodynamics of Non-reacting Fluids* (Edited by B. Le Neindre and B. Vodar), London, Butterworths, 1975, 147-202.
5. David Simpson and Phil Clow of the NPL; initial numerical integration of forces on the ceramic pistons and cylinders; personal communication, 17 August 1995.
6. Note that 35 mm gauges have also been obtained from separate sources and the dimensions of these will be measured as resources permit.
7. Stoup J. R., NIST Precision Engineering Division, personal communication.
8. Dadson R. S., Lewis S. L., Peggs G. N., *The Pressure Balance: Theory and Practice*, London, HMSO, 1982.
9. Prowse D. B., Hatt D. J., *J. Phys. E*, 1977, **10**, 450-451.
10. Sutton C. M., *J. Phys. E*, 1979, **12**, 466-468.
11. Tilford C. R., Hyland R. W., *Proc. XI IMEKO World Congress*, Houston, Texas, 1988; Tilford C. R., *Proc. Workshop and Symposium of the National Conference of Standards Laboratories*, 1988.
12. Delajoud P., Girard M., Ehrlich C. D., Early history of the development and characterization of a 50 mm diameter, gas-operated piston gauge as a primary pressure standard, *Metrologia*, 1999, **36**, 521-524.
13. Driver R. G., Ehrlich C. D., Schmidt J. W., Tison S. A., *Development of Large-diameter Gas-operated Piston Gauge Primary Standards*, Final Report CCG 361, 1996.